

RESEARCH ON DYNAMIC LOAD CARRYING CAPACITY OF ASSEMBLED INTERNAL STIFFENING WIND TURBINE TOWER BASED ON MULTI-SCALE MODELING

Fa-Wu Wang^{*}, Kai-Mming Zhou and Shi-Tang Ke

College of Civil Aviation Engineering Nanjing University of Aeronautics & Astronautics, Nanjing, China

^{*} (Corresponding author: E-mail: fwwang@nuaa.edu.cn)

ABSTRACT

The development of wind power technology requires higher and larger wind turbines, which requires the bearing tower to increase its height and diameter. The assembled internal stiffened wind turbine tower divides the tower into multiple arc plates along the longitudinal direction, which can be easy transported to the site for assembly. That can solve the problem of height limit in highway transportation. At the same time, the internal stiffener provides better stability and can replace the bottom tower section of conventional wind turbine tower. In this study, the tower section of assembled internal stiffened wind turbine is modeled, and the longitudinal segmented tower section is assembled to the actual full-scale tower section model for nonlinear dynamic analysis. The influence of weld is considered by multi-scale modeling, combined with the plastic damage theory of steel materials. The whole collapse process of tower wall instability and deformation failure of wind turbine tower under the extreme wind condition is simulated, and the influence of various parameters of tower section on its bearing capacity is analysed. The damage position and damage development during tower collapse are predicted by using plastic damage theory, so as to provide reference for the design of assembled internally stiffened wind turbine tower.

ARTICLE HISTORY

Received: 20 July 2022
Revised: 22 August 2022
Accepted: 10 January 2023

KEYWORDS

Wind turbine tower;
Multi-scale modelling;
Prefabricated;
Internal stiffening;
Plastic damage

Copyright © 2023 by The Hong Kong Institute of Steel Construction. All rights reserved.

1. Introduction

As a clean and efficient energy, wind power generation has developed very rapidly in recent years, and wind power technology has also developed rapidly. As the main load-bearing component of wind turbine, tower plays an important role in ensuring the stable operation of wind turbine. Considering the height limit of highway transportation, the wind turbine tower with a bottom diameter of more than 4.5m has exceeded the height limit of highway transportation. For the future development of higher power wind turbines, the transportation of larger diameter towers will be a problem. The split assembly towers can well solve the problems of height and width limitation in transportation.

Wind turbine tower belongs to cylindrical shell structure in classification. In the research field of inner stiffened cylindrical shell, Wang M.G. [1] studied the stability of stiffened cylindrical shell by theoretical analysis and Yan H.X. [2] by finite element calculation. It is found that the bearing capacity of non-stiffened shell is the lowest under the action of horizontal wind pressure; The effect of longitudinal stiffening is greater than that of circumferential stiffening, and the effect of external stiffening is better than that of internal stiffening. The longitudinal stiffeners arranged along the height direction can improve the overall stiffness of the tower to a certain extent. Rotter J.M. [3] studied in detail the nonlinear buckling forms of cylindrical shell structures with different lengths under overall bending. Comparing the critical moment calculated by ABAQUS analysis and the critical moment calculated by the traditional calculation formula, it is found that for cylindrical shells with short length, the critical moment at buckling is greater than the elastic critical moment; For medium length cylindrical shells the critical moment is close to the elastic critical moment; For long cylindrical shell structures the buckling critical moment is lower than the elastic critical moment. The influence of boundary conditions on the buckling capacity of long columns is lower than that of short columns.

In this paper, the collapse failure mechanism of wind turbine tower under extreme wind conditions is analysed by considering the assembled internal stiffener and combined with the material plastic damage theory. It is based on the plastic damage theory of stress triaxial [4]. This theory can simulate the fracture phenomenon of materials under different stress states and can predict the collapse failure of large wind turbine structures. Zhou T.H. [5] have used the plastic damage theory to analyze the structural damage of frame joints and steel frame structures under low cycle loading. The results show that the plastic damage theory can accurately predict the degradation of bearing capacity and stiffness of members and steel frame structures under loading, and accurately predict the damage location and damage development of structures. Duan H.X. [6] applied the plastic damage theory to the dynamic time history analysis of steel frame structure, and predicted the failure position and damage development of frame structure under seismic load. As a method to predict the

actual damage of structures, the material plastic damage theory is widely used in the node analysis and collapse analysis of steel frame structures, but there are few applications in the wind turbine tower and the analysis of collapse failure mechanism of the tower. Therefore, the application of material plastic damage theory to the tower structure analysis has practical research significance and value.

At present, scholars have less research on split assembly internal stiffened towers, especially the dynamic bearing performance of such towers and the collapse failure mechanism under extreme conditions need to be furtherly studied. Based on the consideration of fabricated internal stiffening and material plastic damage, this paper studies the dynamic bearing performance of tower under different stiffening schemes, and uses the plastic damage theory to predict the location and development degree of structural damage.

2. Dynamic response analysis of assembled internal stiffener wind turbine

2.1. Simplified finite element model

Taking NREL 5mw wind turbine as the research object, the finite element model is created in ABAQUS. The main parameters of the wind turbine are showed in table 1.

Table 1

Main parameters of NREL 5MW wind turbine

Wind turbine parameters	Numerical value
Diameter of wind turbine/m	126
Hub height/m	90
Tower height/m	87.6
Wind turbine mass/kg	1.1×10^4
Engine room quality/kg	2.4×10^5
Tower mass/kg	3.47×10^5

The bottom diameter of the tower is 6m, the wall thickness is 0.027m, the top diameter of the tower is 3m, and the wall thickness is 0.019m. The shell wall is modeled by shell element SR4. The material is Q355 steel, the density is 7850kg/m^3 , the yield strength is 325MPa, the Poisson's ratio is 0.3, and the elastic modulus is 2.1×10^{11} , the total height of the tower is 87.6m. Taking 8.76m as a tower section, a reference point RP is set on the top of the tower, and the reference point is connected with MPC on the top of the wind turbine tower, the

bottom of the wind turbine tower is rigidly connected with the foundation. For the tower section with a diameter greater than 4.5m, the distribution scheme is adopted, as shown in Fig. 1 (the gray part of the tower section is arranged in pieces). The stiffener is TW75×150 section steel, flange thickness 20mm, Fig. 1 shows the cross section of the tower.

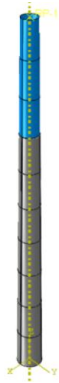


Fig. 1 Simplified finite element model

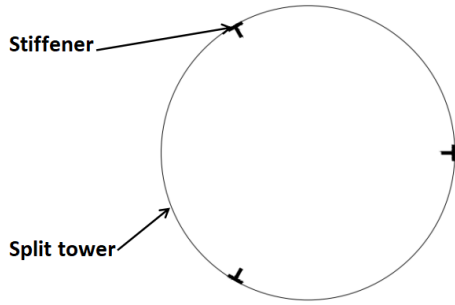


Fig. 2 Schematic diagram of tower section

2.2. Wind load extraction

In this paper, according to the design load condition of wind turbine, the simulation time $T=60s$ and time step $\Delta T=0.1s$ are set by OpenFAST software parameters to calculate the turbulent wind speed under the average wind speed of 70m/s at the hub under the extreme wind condition once in 50 years. The turbulent wind field is generated by TurbSim software to obtain the time domain diagram of wind speed at the hub height, as shown in Fig. 3 extract the wind load time history on the top of the wind turbine tower under the current wind condition, where F_x , F_y and F_z are the axial forces in the X, Y and Z directions respectively, and M_x , M_y and M_z are the moments around the X, Y and Z axes respectively, which is shown in Fig. 4.

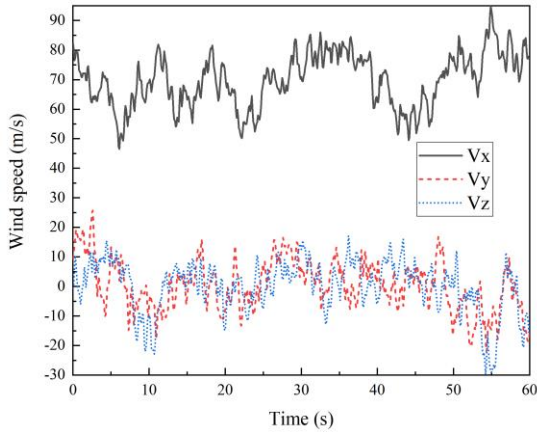
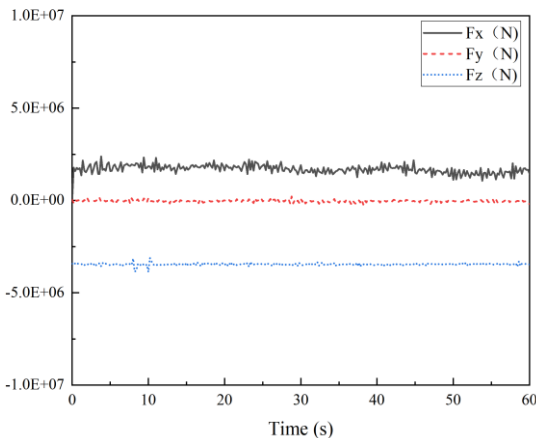
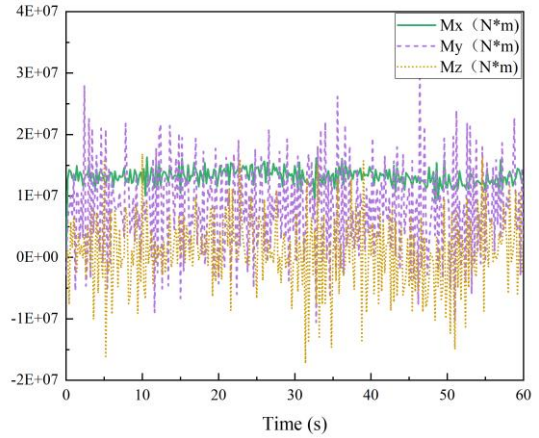


Fig. 3 Wind speed time history at hub



(a) axial forces



(b) moments

Fig. 4 Time history of tower top wind load

2.3. Dynamic buckling failure of tower

Fig. 5 shows the structural Mises stress of instability collapse failure of wind turbine tower under the flange thickness of 20mm and the stiffener is TW 75×150 section steel.

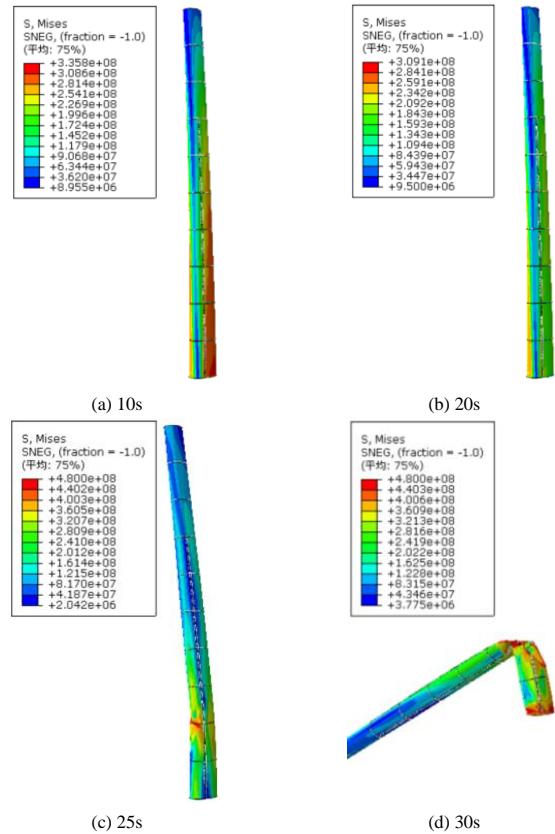


Fig. 5 Stress of wind turbine tower structure at different times

It can be seen from Fig. 5 that the structure has dynamic instability and collapse failure after 20s. The failure position is at the connection of tower section 2 and tower section 3, with an elevation of 17.52m. The section thickness changes greatly here (the section thickness of tower section 2 is 0.027m, and the section thickness of tower section 3 is 0.026m). The stiffness is discontinuous, and dynamic buckling instability is easy to occur.

3. Weld simulation and material plastic damage theory

3.1. Finite element simulation of weld

On the premise of multi-scale modeling, the weld is introduced into the local structure. By comparing with the non-weld model, the influence of the weld on the dynamic collapse of the structure is studied. Here, the inherent strain method is used to simulate the weld. In this paper, the equivalent trapezoidal strain method proposed in reference [7] is used to overcome the problem that the calculation of constant strain method is difficult to converge due to the sudden change of strain field at the edge of the model, as shown in Fig. 6.

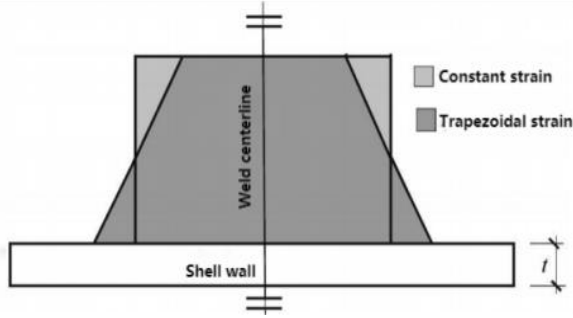


Fig. 6 Schematic diagram of inherent strain method

The 5m tower section at the bottom of a 5MW wind turbine is used for modeling. The tower barrel has a radius of 3m and a thickness of 40mm. The shell element SR4 is used for modeling the wall. The material is Q355 steel with a yield strength of 325MPa. Loading inherent strain value, the tower barrel produces the welding residual stress and deformation allowed by the specification. The comparison between the residual stress distribution along the vertical weld direction of the shell and the measured welding data in reference [8] is shown in Fig. 7. The peak value of residual stress through inherent strain simulation is 320MPa, and the peak value of measured data in reference [8] is 275MPa. The curve is in good agreement within 50mm from the weld line. Although the stress outside 50mm is slightly different, the stress values are small, all less than 50MPa, and the difference is within 25MPa. It can be considered that the inherent strain method can meet the simulation requirements of wind turbine tower weld.

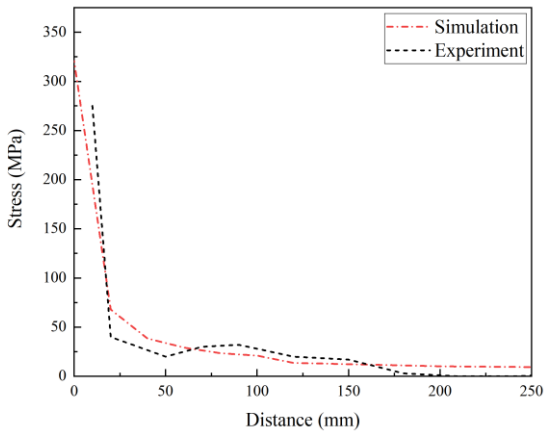


Fig. 7 Comparison of residual stress

3.2. Material micro plastic damage initiation criteria

The internal micro fracture of metal materials is the main reason for the decline of material bearing capacity and stiffness. Due to the expansion of internal micro trauma surface, the effective area of external load borne by metal materials continues to decrease, resulting in the loss of metal material bearing capacity and stiffness. Therefore, for metal materials, the moment of micro fracture in the material is the moment when the material enters the damage state.

Based on Xue and Wierzbicki [9-10] damage criterion as the damage initiation criterion of structural steel, this paper selects the simplified stress triaxial damage initiation criterion suitable for explaining the damage mechanism of structural steel proposed by Li W.C. [11] and Zhou T.H. [5] on the basis of Bao and Wierzbicki [4] equivalent plastic damage strain and stress triaxial path. Through the round bar tensile test of Q355 steel, the plastic damage evolution criterion of steel is determined, so as to provide a suitable material plastic damage theoretical model for the later analysis of the bearing capacity

of wind turbine tower.

Xue and Wierzbicki metal material damage initiation criterion considers that the over accumulated equivalent plastic strain is the main reason for the degradation of stress and stiffness of metal materials. When the equivalent plastic strain of metal material reaches a certain critical value $\bar{\varepsilon}_0^{pl}$, micro fracture occurs in the material, and then enters the plastic damage state. Among them, the critical value of the equivalent plastic strain at the micro fracture time of the material $\bar{\varepsilon}_0^{pl}$ is defined as the equivalent plastic damage strain. How to determine the equivalent plastic damage strain of the material is the main purpose of Xue and Wierzbicki damage initiation criterion. The damage criterion holds that the equivalent plastic damage strain of metal materials $\bar{\varepsilon}_0^{pl}$ is a function of material stress triaxial and stress state parameters:

$$\bar{\varepsilon}_0^{pl} = F(\eta, \xi) \quad (1)$$

$$\eta = \sigma_m / \sigma \quad (2)$$

$$\sigma_m = \frac{1}{3}(\sigma_1 + \sigma_2 + \sigma_3) \quad (3)$$

$$\sigma = \sqrt{\frac{1}{2}[(\sigma_1 - \sigma_2)^2 + (\sigma_2 - \sigma_3)^2 + (\sigma_3 - \sigma_1)^2]} \quad (4)$$

$$\xi = \frac{27 J_3}{2 \sigma^3} \quad (5)$$

Where, σ_m and σ are hydrostatic stress and Mises equivalent stress of the material. σ_1 , σ_2 , σ_3 respectively is the principal stress in three directions of the material; J_3 is the third deviatoric stress which can be expressed as:

$$J_3 = \sigma_1 \sigma_2 \sigma_3 \quad (6)$$

In Bao and Wierzbicki damage criterion, the damage strain function needs to be calibrated by the fracture of various notch specimens. Yu [12] simplified the path of steel stress triaxial and equivalent plastic damage strain through analysis, removed the parameter under the premise of ensuring accuracy, and greatly reduced the difficulty of determining the parameters, The simplified material equivalent plastic damage strain can be expressed as follows.

$$\bar{\varepsilon}_0^{pl} = \begin{cases} \infty \\ C_1 / (1 + 3\eta) \\ C_1 + (C_2 - C_1)(\eta / \eta_0)^2 \\ C_2 \eta_0 / \eta \end{cases} \quad (7)$$

Where η_0 is the limit value of the fracture performance of the material in high stress triaxial and low stress triaxial, C_1 and C_2 is the material parameter. From the formula, it can be seen that the plastic damage strain of material can be expressed as a piece-wise function of stress triaxial. The conversion relationship between C_1 and C_2 is shown in formula (8). C_2 is the equivalent plastic strain of the material round bar specimen during uniaxial tensile fracture, the parameters can be determined by testing the reduced area A_R of the section at the fracture of the smooth round bar specimen. K , n is the material hardening parameter, which can be calculated from the material stress-strain curve.

$$C_1 = C_2 (\sqrt{3}/2)^{1/n} \quad (8)$$

$$C_2 = -\ln(1 - A_R) \quad (9)$$

$$\sigma = K(\varepsilon)^n \quad (10)$$

The simplified curve path of equivalent plastic damage strain and stress triaxial of steel is shown in Fig. 8.

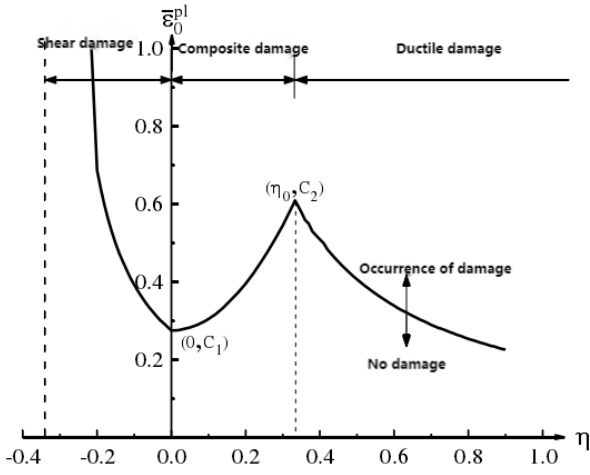


Fig. 8 Stress triaxial and equivalent plastic damage strain path

3.3. Micro plastic damage evolution of materials

The material plastic damage initiation criterion only gives the equivalent plastic strain position when the steel damage occurs, but does not give the stress decline path after the damage occurs. After the steel enters the damage stage, the bearing capacity and stiffness of the material decay, and the damage factor can represent the attenuation degree of the material stress and elastic modulus. Therefore, the relationship between material residual stress, residual elastic modulus and damage factor D can be expressed by the following formula:

$$\bar{\sigma} = (1 - D)\sigma \quad (11)$$

$$\bar{E} = (1 - D)E \quad (12)$$

It can be seen from formulas 11 and 12 that when the damage factor $D=0$, the material does not enter the damage state, and the stiffness and bearing capacity of the material do not degrade. When $D>0$, the material begins to enter the damage state, and the stiffness and bearing capacity of the material degrade. When $D=1$, the steel is destroyed. At this time, the residual modulus and residual stress of the material are reduced to 0. The damage factor function of steel is determined through the round bar tensile test of steel, and the material plastic displacement and failure plastic displacement \bar{u}^{pl} are introduced to determine the damage factor D . the difference between the total tensile displacement and elastic displacement of the member is defined as the plastic displacement \bar{u}^{pl} , the plastic displacement when the member is completely damaged is defined as the failure plastic displacement \bar{u}_f , and the damage factor D can be expressed as the function of \bar{u}^{pl}/\bar{u}_f :

$$D = F(\bar{u}^{pl}/\bar{u}_f) \quad (13)$$

Reference [13] once expressed the damage factor D as a linear function of \bar{u}^{pl}/\bar{u}_f . This method has obvious approximation. After the steel specimen reaches the peak stress, there will be obvious necking phenomenon, which is reflected in that the decline path after the steel tensile peak stress is not a straight line, but an approximate power exponential curve. Through the tensile test of Q355 steel round bar in document [13] and the fitting of the function of steel damage factor D by Zhou T.H. [4], the damage factor D can be expressed as the power function of the ratio of plastic displacement to ultimate failure displacement of Q355 steel:

$$D = 1.3 \left(\frac{\bar{u}^{pl}}{\bar{u}_f} \right)^{7.6} \quad (14)$$

According to the above material plastic damage theory, the values of material parameters are as follows:

$$n=0.189, K=876\text{MPa}, C_1=0.293, C_2=0.63, \eta_0=1/3, \bar{u}=0.02\text{m}$$

4. Damage and collapse mechanism analysis of wind turbine based on multi-scale modeling

4.1. Development of wind turbine damage

Due to the introduction of fatigue damage theory in the model, the local damage location and development degree of the wind turbine under extreme wind conditions can be predicted. With the continuous accumulation of material equivalent plastic strain, some elements finally reach the equivalent plastic strain at the initial damage, and then enter the damage state. Then, the bearing capacity of the damaged elements begins to deteriorate, which is manifested by the increase of damage factor D . The DUCTCRT index in ABAQUS is the damage initiation index of the material, which is used to determine the damage state of the element. If the parameter is equal to 1, it indicates that the element enters the damage state; The SDEG index is the damage factor D , which is used to measure the degradation degree of the stiffness and strength of the material. This index is 1, indicating the complete loss of the stiffness and strength of the material, which can basically be regarded as the fracture of the material.

Fig. 9 and Fig. 10 shows the structural damage development distributions of the two models with increasing time in dynamic time history analysis are given. From Fig. 9 it can be seen that the damage of the weld model first appears in the weld area. With the passage of time, the damage area will expand circumferentially along the weld, and the damage at the weld is particularly obvious. The DUCTCRT index of the damage state will be further increased on the original basis. With the passage of time, the DUCTCRT index of the weld area will reach 1, and most of the structure will be damaged. The damage is concentrated in the weld area. From Fig. 10 it can be seen that due to the large change of section stiffness the dynamic buckling damage is easy to occur. With the passage of time, the structural damage area gradually expands, and the damage is mainly concentrated at the connection of tower section. The damage location of the structure is basically consistent with the buckling failure location.

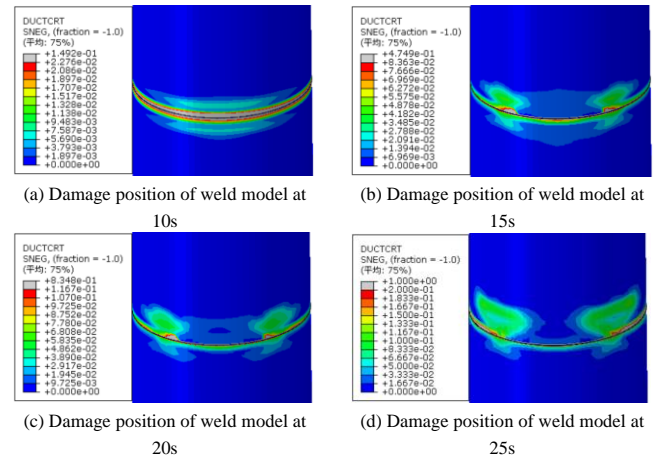


Fig. 9 Development of damaged parts of weld model

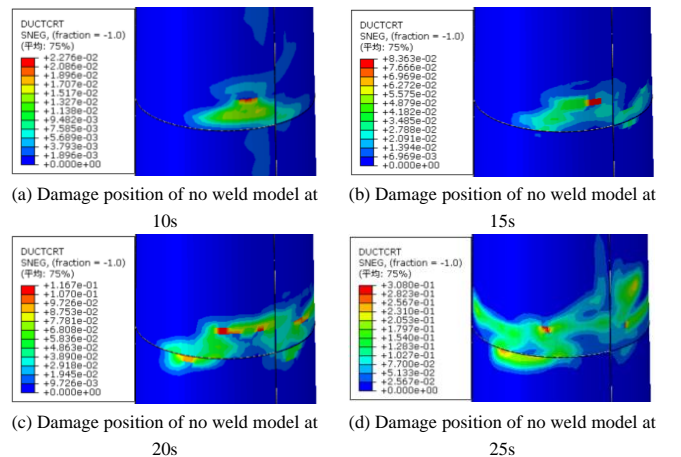


Fig. 10 Development of damaged parts of no weld model

In terms of the damage development speed, the weld of the weld model enters the damage state fastest, mainly because a certain plastic strain has been accumulated at the weld, so it can enter the damage state faster.

In order to compare the influence of welds on the degree of structural damage, Fig. 11 shows the comparison of structural damage factor SDEG under

different models. There are obvious differences in structural damage at the weld. According to the damage factor SDEG index, the stiffness and elastic modulus of the weld model are completely degraded along the weld at 25 seconds, which can be approximately considered that the structure is cracked, while the material is not completely degraded without the weld model at 25 seconds.

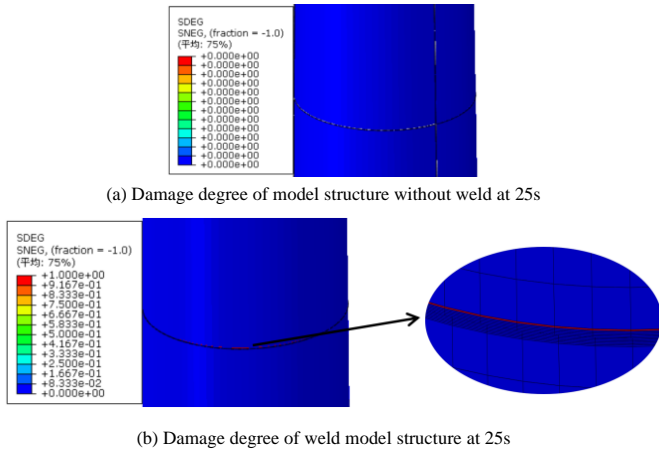


Fig. 11 Comparison of damage degree

4.2. Stiffener damage development

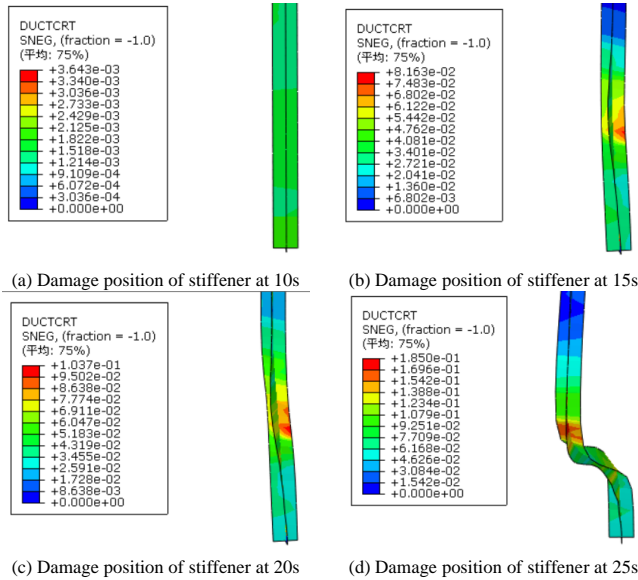


Fig. 12 Stiffener damage development

Fig. 12 shows the development of stiffener damage with the increase of load time history in the weld model. It can be seen from the figure that the damage of stiffener is mainly concentrated in the connection position of tower, and there will be no damage in other positions. With the increase of wind load time history, the deformation and damage of stiffener also increase. At 25s, the DUCTCRT value of tower structure reaches 1, while the stiffener is only 0.185, indicating that the damage degree of tower is much greater than that of stiffener at the same time. Considering that the size of the stiffening rib under this stiffening scheme is small, the stiffening effect on the tower is not obvious.

5. Conclusions

With the aim to investigate the dynamic load carrying capacity and the collapse failure mechanism of wind turbine tower with assembled internal stiffening, this paper analyzed the influence of weld by multi-scale modeling, combined with the plastic damage theory of steel materials. The following points were concluded:

1) The damage position of weld model and non weld model is basically the same as that of structural dynamic buckling failure. The damage of weld model is mainly concentrated in the area near the weld, and the damage of non-weld model is mainly concentrated in the position where the variable section stiffness of tower is discontinuous.

2) With the increase of wind load time history, the area of structural damage area also increases gradually. The weld model develops along the weld circumferential direction, and the damage at the weld develops the fastest. The non-weld model shows irregular damage development at the discontinuity of structural stiffness, and the damage degree of the weld model is greater than that of the non weld model at the same time.

3) The stiffener at the connection of tower and tube will be damaged first, and the rest will not be damaged. With the increase of wind load time history, the deformation and damage of stiffener will also increase. At the same time, the damage degree of stiffener is much less than that of tower and tube.

Acknowledgments

This project is jointly supported by Projects of International (Regional) Cooperation and Exchanges NSFC (52211530086) and Jiangsu Provincial Science Fund for Distinguished Young Scholars (BK20211518), the opinions, findings, and conclusions or recommendations expressed in this paper are those of the authors and do not necessarily reflect the views of the sponsors.

References

- [1] Wang M.G., Huang Y., "Study on wind stability of two-way multi ribbed shell structure", Engineering mechanics, 2000 (04): 44-49.
- [2] Yan H.X., "Combined with an example, the local stability of large diameter tower is studied", Special structure, 2014,31 (04): 41-47.
- [3] Rotter J.M., Sadowski A.J., Chen L., "Nonlinear stability of thin elastic cylinders of different length under global bending", International Journal of Solids & Structures, 2014, 51(15-16): 2826-2839.
- [4] Bao Y., Wierzbicki T., "On fracture locus in the equivalent strain and stress triaxiality space", International Journal of Mechanical Sciences, 2004, 46(1): 81-98.
- [5] Zhou T.H., Li W.C., Guan Y., Bai L., "Damage analysis of steel frame under cyclic loading based on stress triaxiality", Engineering mechanics, 2014,31 (07): 146-155.
- [6] Duan H.X., Li S.J., Liu Y.X., "Numerical simulation of damage process of steel structure under earthquake", Engineering mechanics, 2011,28 (02): 198-204.
- [7] Hübner A., Teng J.G., and Saal H., "Buckling behavior of large steel cylinders with patterned welds", International Journal of Pressure Vessels and Piping, 2006, 83: 13-26.
- [8] Yang N., Lin S., Su C., "Study on residual stress and damage distribution of thick plate welded joints", Journal of Hunan University (Natural Science Edition), 2014,41 (11): 24-31.
- [9] Wierzbicki T., Xue L., "On the effect of the third invariant of the stress deviator on ductile fracture", Cambridge, MA, USA: MIT Impact and Crashworthiness Lab, 2005.
- [10] Xue L., "Damage accumulation and fracture initiation in uncracked ductile solids under triaxial loading—Part I: Pressure sensitivity and Lode dependence", Cambridge, MA, USA: MIT Impact and Crashworthiness Lab, 2005.
- [11] Li W.C., Zhou T.H., Liao F.F., Lu Y., "Application of ductile damage criterion in dynamic time history analysis of steel frame structures", Building structure, 2018, 48 (22): 21-27.
- [12] Yu H.L., Jeong D.Y., "Application of a stress triaxiality dependent fracture criterion in the finite element analysis of unnotched Charpy specimens", Theoretical and Applied Fracture Mechanics, 2010, 54(1): 54—62.
- [13] Fang F.L., Wang W., Chen Y.Y., "Experimental Study to Calibrate Monotonic Micro mechanics-Based Fracture Models of Q345 Steel", Advanced Materials Research, 2011, 1278(524):545-550.